

Monte Carlo Study of Detector Concepts for the MAX Laue Lens Gamma-Ray Telescope

G. Weidenspointner¹, C.B. Wunderer², N. Barrière¹, A. Zoglauer², and P. von Ballmoos¹

¹ Centre d'Etude Spatiale des Rayonnements, 9 Avenue Colonel Roche, 31028 Toulouse Cedex 4, France

² Space Science Laboratory, UC Berkeley, Berkeley, USA

Received ; accepted

Abstract. MAX is a proposed Laue lens gamma-ray telescope taking advantage of Bragg diffraction in crystals to concentrate incident photons onto a distant detector. The Laue lens and the detector are carried by two separate satellites flying in formation. Significant effort is being devoted to studying different types of crystals that may be suitable for focusing gamma rays in two 100 keV wide energy bands centered on two lines which constitute the prime astrophysical interest of the MAX mission: the 511 keV positron annihilation line, and the broadened 847 keV line from the decay of ⁵⁶Co copiously produced in Type Ia supernovae. However, to optimize the performance of MAX, it is also necessary to optimize the detector used to collect the source photons concentrated by the lens. We address this need by applying proven Monte Carlo and event reconstruction packages to predict the performance of MAX for three different Ge detector concepts: a standard coaxial detector, a stack of segmented detectors, and a Compton camera consisting of a stack of strip detectors. Each of these exhibits distinct advantages and disadvantages regarding fundamental instrumental characteristics such as detection efficiency or background rejection, which ultimately determine achievable sensitivities. We conclude that the Compton camera is the most promising detector for MAX in particular, and for Laue lens gamma-ray telescopes in general.

Key words. gamma-rays, Laue lens, germanium detectors, Compton telescopes, nuclear lines, positron annihilation

1. Introduction

Gamma-ray lines carry unique information of prime importance for our understanding of fundamental astrophysical questions such as the origin of heavy elements or the mechanisms behind the spectacular death of stars in supernovae (see e.g. reviews by Prantzos 2005; Weidenspointner 2006). Despite their paramount interest, observations of gamma-ray lines have historically been plagued by intense and complex instrumental backgrounds against which the much smaller signals from celestial sources need to be discerned (e.g. Weidenspointner et al. 2005). Recently, a novel experimental technique, promising to improve the sensitivity of existing gamma-ray telescopes by one to two orders of magnitude, has been demonstrated: the Laue lens (Halloin et al. 2004; von Ballmoos et al. 2004).

A Laue lens takes advantage of Bragg diffraction in crystals to concentrate incident gamma rays onto a detector (Lund 1992; Smither et al. 1995; Halloin et al. 2004; von Ballmoos et al. 2004). In this approach it is possible to employ a large photon collecting area together with a

small detector volume, which results in a greatly increased signal-to-background ratio and hence a greatly improved sensitivity.

MAX is a Laue lens telescope that has been proposed to the French Space Agency CNES in response to an announcement of opportunity for a formation flight demonstration mission (Barrière et al. 2006; von Ballmoos et al. 2006). The MAX gamma-ray Laue lens consists of Ge and Cu crystals and has a focal length of about 86 m. MAX is designed to concentrate gamma rays in two 100 keV wide energy bands centered on the two lines which constitute the prime astrophysical interest of the mission: the 511 keV positron annihilation line, and the broadened 847 keV line from the decay of ⁵⁶Co copiously produced in Type Ia supernovae.

Significant effort is being devoted to studying different types of crystals that may be suitable for focusing gamma rays at nuclear line energies (e.g. Abrosimov et al. 2006; Courtois et al. 2006; Smither et al. 2006). However, to achieve the best possible performance of MAX, it is also necessary to optimize the detector used to collect the source photons concentrated by the lens. We address this need by applying proven Monte Carlo and event reconstruction packages to predict the performance of MAX for

three different Ge detector concepts: a standard co-axial detector, a stack of segmented detectors, and a Compton camera consisting of a stack of strip detectors. We chose Ge as detector material since it provides the best energy resolution for line spectroscopy in the energy range of nuclear transitions. Each of these detector concepts exhibits distinct advantages and disadvantages regarding fundamental instrumental characteristics such as detection efficiency or background rejection, which ultimately determine achievable sensitivities. Our goal is to identify the most promising detector concept for a Laue lens. We consider the expected sensitivity to be the most important performance parameter, but also include capabilities for spectroscopy, imaging, and polarimetry in our final decision. The most promising detector concept will be studied in more detail and optimized in the future. First advances in the design of a Compton detector are presented in a companion paper by Wunderer et al. (2006b).

2. Simulation of instrument performance

This section provides a brief overview of the simulation and analysis techniques that we employed to estimate by *ab initio* Monte Carlo simulation the performance of three different detector concepts for MAX. Our study benefited from experience gained from the modelling of the performance of past or existing gamma-ray missions such as TGRS on board *Wind*, the Ramaty High Energy Solar Spectroscopic Imager (*RHESSI*), or SPI onboard *INTEGRAL* by Monte Carlo simulation (see Weidenspointner et al. 2005; Wunderer et al. 2004; Weidenspointner et al. 2003, respectively), and the enhanced set of Monte Carlo and data analysis tools developed for predicting the performance of various instrumental concepts for a future *Advanced Compton Telescope* (Wunderer et al. 2006a; Boggs et al. 2006a).

2.1. Instrument and spacecraft models

Among other inputs, the simulation of the performance of a gamma-ray instrument requires a detailed computer description of the experimental set-up under study. This so-called mass model specifies the geometrical structure of instrument and spacecraft, the atomic and/or isotopic composition of materials, and sets parameters that influence the transport of particles in different materials.

The basic design of the MAX detector spacecraft and the mounting and cooling of the detector concepts assumed in this study emerged from the CNES pre phase A study of the MAX mission (Barrière et al. 2006; von Ballmoos et al. 2006). This basic design is identical for all three detector concepts, the only difference between the mass models is in the definition of the detectors. As can be seen in Fig. 1, in each concept the detector is located on top of a 1 m tower; passive cooling is provided by a Be radiator of diameter 1 m. The dimensions of the cylindrical spacecraft body are radius 60 cm and height 192 cm. The spacecraft contains, among other components, tanks

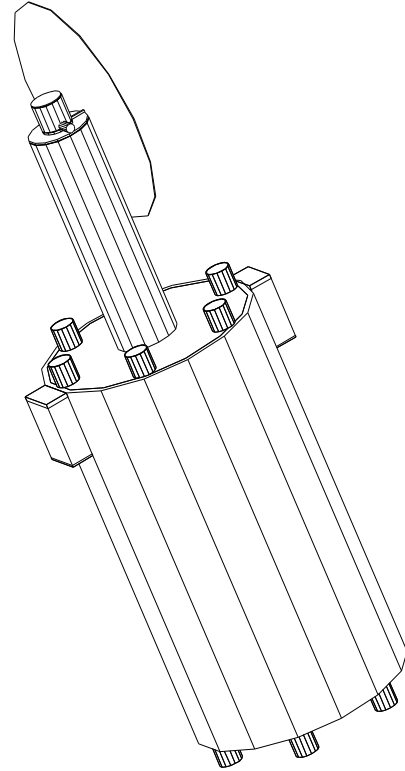


Fig. 1. A side view of the MAX detector spacecraft model. The spacecraft body is cylindrical. The detector is situated on top of a 1 m tower. The circular radiator assumed to passively cool the detector is clearly visible. Details are given in the text.

for hydrazine propellant and for cold gas, various electronics boxes, reaction wheels, and thrusters. The total mass of the spacecraft is about 260 kg. The tower separating the detector from the spacecraft body is intended to reduce possible instrumental background created in the satellite structure. In addition, a 5 cm thick BGO (bismuth germanate) crystal at the top of the tower and underneath the detector (see Figs. 2 and 3) serves as active (veto) and passive shield for the detector. The combined mass of the tower structure, the BGO veto shield, the radiator, and various detector electronics components is about 47 kg.

To study the performance of a standard co-axial detector concept for MAX (hereafter: MAX-TGRS) we resorted to the TGRS Ge detector flown on the *Wind* mission. The TGRS detector has been described by Owens et al. (1995); our mass model is a modified version of the TGRS mass model used by Weidenspointner et al. (2005) for their detailed instrumental background study. A section of the MAX-TGRS detector mass model, including the top of the tower, is depicted in Fig. 2. Size, geometry, and material composition of Ge crystal, cathode, and Al housing remained unchanged. For MAX-TGRS, the radiative cooler of the original TGRS detector was removed. Instead, a cold finger leading to the radiator was introduced, and

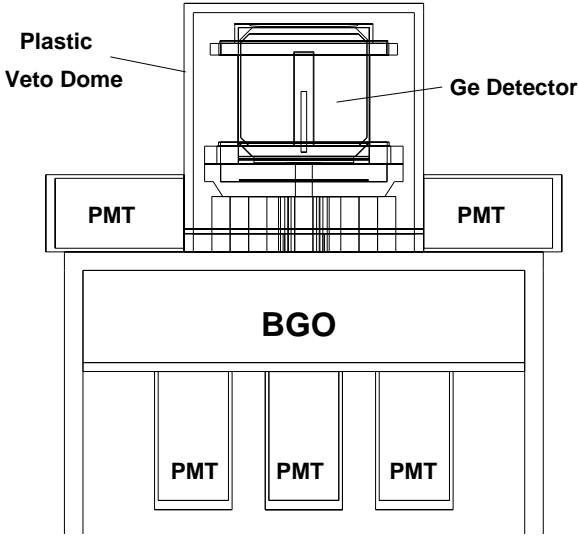


Fig. 2. A section of the MAX-TGRS detector mass model, including the top of the tower. The Ge crystal is surrounded by a plastic veto dome at the sides and at the top, and by a BGO crystal at the bottom.

miscellaneous passive materials representing assumed detector support structure and electronics were positioned below the detector housing. The detector assembly is enclosed on the sides and at the top by a 0.5 cm thick plastic veto shield, which is viewed by two photomultipliers (PMTs). Also depicted in Fig. 2 are the BGO veto shield beneath the detector assembly and the respective PMTs. Plastic dome and BGO crystal cover all lines of sight to the Ge crystal. The volume of the Ge crystal (height about 6.1 cm, radius about 3.4 cm) is about 216 cm^3 , the total mass of the detector assembly including the plastic veto dome is about 3 kg.

The performance of a stack of segmented detectors and of a Compton camera consisting of a stack of strip detectors was studied with the exact same mass model, but different analysis procedures for the simulated data (see Sec. 2.6). Both the segmented (hereafter: MAX-NCTseg) and the Compton detector (hereafter: MAX-NCTcompt) concepts consist of a stack of five detector modules modelled after the successfully tested Ge detectors of the balloon borne *Nuclear Compton Telescope* (NCT Boggs et al. 2006b). As can be seen in Fig. 3, the basic layout of the instrument geometry (or mass model) for these two concepts is the same as that of MAX-TGRS: the detector assembly is located inside a plastic veto dome, with the BGO veto shield below. Each of the five detector planes is roughly $8 \times 8 \text{ cm}^2$ in size, with a thickness of 1.5 cm, yielding a total detector volume of about 480 cm^3 . The gap between adjacent detector planes was chosen to be 0.7 cm in our concepts. The total mass of the detector assembly including the plastic veto dome is about 6 kg.

Each of these detector concepts exhibits distinct advantages and disadvantages. From a technical point of view, the MAX-TGRS concept is simplest and easiest to

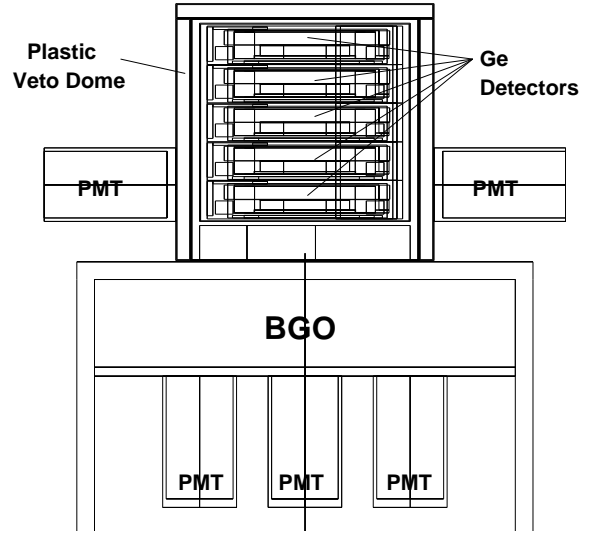


Fig. 3. A section of the MAX-NCTseg and MAX-NCTcompt detector mass models, including the top of the tower. The stack of Ge detectors is surrounded by a plastic veto dome at the sides and at the top, and by a BGO crystal at the bottom.

realize, while MAX-NCTcompt is the most complex and demanding. MAX-TGRS has only one detector channel, MAX-NCTseg a few, MAX-NCTcompt a few hundred; consequently cooling MAX-NCTcompt is much more challenging than MAX-TGRS. MAX-NCTcompt offers superior background rejection capabilities, at the price of reduced photopeak efficiency, because much more information is available for each registered event than for the other two concepts.

Finally, MAX-NCTcompt has the unique advantage of fine spatial resolution, which is indispensable for realizing imaging and polarimetry.

We would like to emphasize that all three detector concepts are conservative in the sense that we only used detector designs that have already been flown and successfully operated in a space environment. However, the design of all three concepts can be improved, e.g. by minimizing the amount of passive materials, by carefully selecting the passive materials (e.g. elemental composition: carbon fiber instead of Al structure), or by optimizing the geometry and amount of detector material for the photon energies of interest to MAX. This is particularly pertinent for the NCT detectors, which currently are designed with emphasis on cost as well as reliability and robustness for use in a balloon demonstration flight. We therefore expect our performance estimates to be conservative, and that improvements of the detector designs will result in improved performance.

2.2. Lens beam and effective area

Estimating the performance of MAX detector concepts also requires a model for the focal spot distribution of

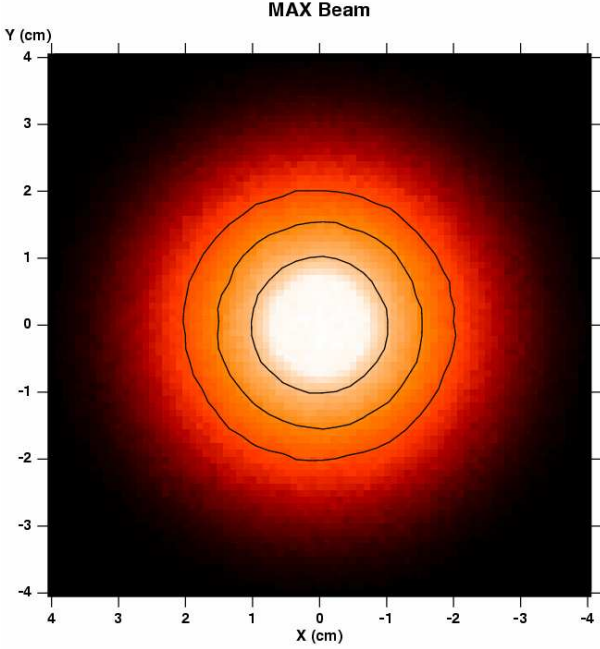


Fig. 4. The focal spot distribution of photons concentrated by the MAX Laue lens onto the detector plane. The three contour levels indicate, with increasing radius, the detector surface exposed to 50%, 75%, and 90% of all incident photons, respectively. More details are given in the text.

photons concentrated by the Laue lens, and an estimate of its effective area (i.e. the geometrical area times the diffraction efficiency). For this study, both quantities were determined by Monte Carlo simulation. As described in more detail in Barrière et al. (2006), for this study the lens crystals were assumed to have a geometrical size of $1.5 \text{ cm} \times 1.5 \text{ cm}$ and a mosaicity of $30''$. The focal length was assumed to be 86 m, and the source was assumed to be located on the optical axis (i.e. the lens is pointed at the source).

For these parameters, about 50% of the photons from an on-axis point source that are diffracted by the lens are concentrated within 1 cm from the center of the focal spot, as can be seen in Fig. 4 depicting the simulated focal spot distribution. To actually perform the detector response simulations in our study, the Laue lens focal spot distribution was introduced as a new beam type named **LRAD** into the MGGPOD Monte Carlo suite described below in Sec. 2.4. Unlike the focal spot distribution of the Laue lens design considered here, the effective area of the lens is a function of energy: about 1191 cm^2 and 661 cm^2 at energies of 511 keV and 847 keV, respectively.

2.3. Radiation environment models

In the CNES pre phase A study it was concluded that MAX would be best operated in either a high Earth orbit (HEO) or an L2 orbit (von Ballmoos et al. 2006). The in-

strumental background would then mainly be due to two radiation fields, namely diffuse cosmic gamma rays and Galactic cosmic rays. Both radiation fields were assumed to be isotropic in our simulations. The spectrum of the diffuse cosmic gamma-ray background was taken from the analytical description given by Gruber et al. (1999). The spectrum and intensity of Galactic cosmic-ray protons was modelled using the COSN default solar minimum spectrum of the MGGPOD package, which is based on the cosmic-ray propagation models of Moskalenko et al. (2002).

Galactic cosmic rays not only produce prompt background due to hadronic interactions and de-excitations of excited nuclei, but also produce radioactive isotopes whose decay gives rise to delayed instrumental background. When simulating this delayed background, we assumed that the instrument and spacecraft materials had been irradiated for one year with the COSN cosmic-ray proton spectrum and intensity.

2.4. MGGPOD Monte Carlo suite

We used the MGGPOD Monte Carlo package (Weidenspointner et al. 2005) to simulate the response and the instrumental background expected for each of the three different detector concepts for MAX. MGGPOD is a user-friendly suite of Monte Carlo codes that is available to the public from a site at CESR¹. MGGPOD is built around the widely used GEANT3.21 package (Brun 1995) and allows simulation *ab initio* of the physical processes relevant for estimating the performance of gamma-ray instruments. Of particular importance is the production of instrumental backgrounds, which include the build-up and delayed decay of radioactive isotopes as well as the prompt de-excitation of excited nuclei, both of which give rise to a plethora of instrumental gamma-ray background lines in addition to continuum backgrounds. Among other packages, MGGPOD includes the GLECS (Kippen 2004) and GLEPS (McConnell & Kippen 2004) packages for simulating the effects of atomic electron binding and photon polarization for Rayleigh and Compton scattering.

As mentioned in Sec. 2.2, for this study a new beam type named **LRAD** was introduced into the MGGPOD Monte Carlo suite. This beam allows the user to define an azimuthally symmetric incident photon flux which is characterized by its radial profile. The direction of incidence is assumed to be identical for all photons, rather than spread over the directions to the lens covering a few degrees in the field-of-view, which is an approximation that should not significantly affect our detector performance estimates at this early stage of the study.

2.5. MEGAlib analysis package

The complex event analysis for the MAX-NCTcompt detector concept was performed with the MEGAlib package (Zoglauer et al. 2006). Originally, it had been de-

¹ <http://sigma-2.cesr.fr/spi/MGGPOD/>

veloped for the MEGA Compton telescope prototype (Kanbach et al. 2004). The package provides the complete data analysis chain for Compton telescopes, including the crucial steps of event reconstruction and background rejection, which are described in more detail in Zoglauer (2005); Zoglauer et al. (2006); Wunderer et al. (2006b) and references therein.

2.6. Data analysis

We compared the performance of the three MAX detector concepts under study for three different gamma-ray lines: narrow lines at 511 keV and 847 keV, and a broadened line (3% full width at half maximum, FWHM, deemed typical for Type Ia supernovae) at 847 keV. For each concept we simulated the instrumental response to these three lines for an on-axis point source. We also simulated the instrumental backgrounds due to diffuse cosmic gamma rays, to Galactic cosmic-ray protons at solar minimum, and to the decay of radioactive isotopes resulting from one year of cosmic-ray proton irradiation. For all three concepts radioactive decays in the detectors and diffuse cosmic gamma rays were found to be the dominant instrumental background components. In comparison, the prompt cosmic-ray induced background is small, and the background due to radioactive decays in the satellite structure is even smaller.

Despite the fact that source photons are concentrated by the Laue lens onto the detector, MAX is still largely background dominated (the signal-to-noise ratio being on the order of several per cent), and we calculated its sensitivity to an on-axis gamma-ray line point source according to

$$f_{n_\sigma} = \frac{n_\sigma \cdot \sqrt{\sum_{i=1}^{n_b} b_i(\Delta E)}}{A_{\text{eff}} \cdot \epsilon(\Delta E) \cdot \sqrt{t_{\text{tot}}}} \cdot \eta \quad (1)$$

where f_{n_σ} is the sensitivity in [$\text{ph cm}^{-2} \text{s}^{-1}$], n_σ is the statistical significance of the detection, $\sum_{i=1}^{n_b} b_i(\Delta E)$ is the sum of all instrumental background components in [cts s^{-1}] in the analysis interval ΔE centered on the line energy, A_{eff} is the effective area of the Laue lens in [cm^2], $\epsilon(\Delta E)$ is the photopeak efficiency, t_{tot} is the total effective observation time in [s], and η is a factor in the range 1–2 whose value depends on how the instrumental background during an observation is determined. Ideally, the instrumental background is known, and η becomes 1. If the instrumental background is determined through an on-off observation strategy, i.e. one half of the total effective observation time is spent pointing at the source, and the other half pointing away from the source measuring the instrumental background, η is 2. An intermediate case can be realized by operating two detectors simultaneously such that they alternately point at the source and away from it; η then assumes a value of $\sqrt{2}$.

For MAX-TGRS data analysis is straight forward since the only event selections that can be applied in the case of a single detector crystal are the thresholds of the detector and of the veto shields and the width of the analysis

energy interval. We assumed the same thresholds for all three concepts: 15 keV for the detector, and veto thresholds of 70 keV and 200 keV for the BGO and plastic dome shields, respectively. We assumed an energy resolution as measured for the SPI detectors (Lonjou et al. 2005) for the MAX-TGRS detector. In the MAX-TGRS concept it is impossible to separate source signal and instrumental background from a single observation; an on-off pointing strategy must be adopted, and $\eta = 2$ in Eq. 1 when calculating the instrument sensitivity. At best, two MAX-TGRS detectors could be operated simultaneously; the minimum value of η therefore is $\sqrt{2}$ for this concept.

For MAX-NCTseg, data analysis is slightly more complicated. As described in Sec. 2.2, for an on-axis point source the Laue lens concentrates source photons onto a relatively small focal spot. This can be exploited in the data analysis by including the criterion that a valid event must deposit energy in a cylindrical detector volume centered on the optical axis in a selected set of detector layers; events that do not deposit energy in these central detector volumes are most likely instrumental background that should be rejected. We implemented this simple scheme by assuming that each detector layer consists of two segments or pixels: a cylindrical, central segment, and a second segment comprising the remaining detector layer volume. Different values for the central radius were tried. In addition, we varied in the analysis the number of detector layers used to record source photons (source recording detector layers – SRDLs) in order to estimate the optimum number of detector layers for the MAX-NCTseg concept without performing a full simulation for each possibility. In doing so, we also had to choose how to treat remaining detector layers (background recording detector layers – BRDLs): these were either ignored or used as additional veto shields. A valid event was required to deposit more than 15 keV in at least one central pixel of the SRDLs without any veto trigger. We assumed an energy resolution as measured for the NCT detectors (S. Boggs, priv. comm.). For the same reasons given for the MAX-TGRS concept, η lies in the range $\sqrt{2}$ –2 for the MAX-NCTseg concept.

Data analysis for MAX-NCTcompt was most complex and performed using MEGAlib. Many logical criteria can be applied to decide whether the energy deposits in the detector are consistent with an interaction sequence of a photon originating from the Laue lens, including the criterion that the first interaction needs to occur in a cylindrical detector volume of a given radius centered on the optical axis in any one of a selected set of detector layers (see Wunderer et al. 2006b, for details). The spatial pitch of the Ge strip detectors was assumed to be 2 mm in the plane of the detectors, and 0.4 mm in depth (S. Boggs, priv. comm.). Again, we assumed an energy resolution as measured for the NCT detectors. The inherent imaging capabilities of the MAX-NCTcompt detector should permit both the source signal and the instrumental background to be measured in a single observation, as was the case for the imaging Compton telescope COMPTEL

Table 1. The sensitivity of three detector concepts for MAX for three different gamma-ray lines. Sensitivities are for a statistical significance of 3σ and a total effective observation time of 10^6 s. The effective area of the MAX Laue lens was assumed to be 1191 cm^2 and 661 cm^2 at 511 keV and 847 keV, respectively. The quoted values pertain to the energy interval ΔE , centered on the line energy, that optimizes the sensitivity. The ranges in sensitivity reflect the possible values of η in Eq. 1 as discussed in the text. The range in sensitivity for MAX-NCTseg in addition includes the two choices for treating energy deposits in unused detectors, which may be ignored or used as additional veto.

	MAX-TGRS	MAX-NCTseg	MAX-NCTcompt
Line Energy [keV]	Sensitivity [$10^{-6} \text{ ph/cm}^2/\text{s}$]		
511	4.2–6.0	2.5–4.6	1.3–1.8
847	4.9–6.9	2.6–3.8	1.3–1.8
847 (3% FWHM)	18–25	10–15	3.5–4.9

Table 2. The photopeak efficiencies and the background rates that went into the calculation of the line sensitivities in Table 1.

	MAX-TGRS	MAX-NCTseg	MAX-NCTcompt
Line Energy [keV]	Photopeak Efficiency [%]		
511	38	22 – 28	6
847	24	16 – 22	6
847 (3% FWHM)	27	17 – 24	6
Line Energy [keV]	Background Rate [cts/s]		
511	2.1×10^{-1}	$2.3 \times 10^{-2} - 6.5 \times 10^{-2}$	1.0×10^{-3}
847	3.4×10^{-2}	$4.2 \times 10^{-3} - 8.6 \times 10^{-3}$	2.6×10^{-4}
847 (3% FWHM)	5.2×10^{-1}	$8.0 \times 10^{-2} - 1.6 \times 10^{-1}$	2.1×10^{-3}

(Schönfelder et al. 1993). Any need for off-source observations is therefore obviated, and the total effective observation time t_{tot} can be spent pointing at the source. In this case the value of η approximates 1 in Eq. 1. An exact determination of the value of η is difficult and beyond the scope of this paper. We expect the number of data space bins free of source signal to exceed that of data space bins containing source signal, hence η should be smaller than $\sqrt{2}$. We conservatively adopt a range of $1-\sqrt{2}$ for η for the Compton detector concept.

3. Results

The sensitivities of the three different MAX detector concepts for an on-axis point source for three different gamma-ray lines are summarized in Table 1. Sensitivities are for a statistical significance of 3σ and a total effective observation time of 10^6 s; the ranges reflect the possible values of η in Eq. 1 as discussed above. The effective area of the MAX Laue lens was assumed to be 1191 cm^2 and 661 cm^2 at 511 keV and 847 keV, respectively. Sensitivity values are quoted for the best choices of both the radius

of the central pixel and of the width of the energy interval ΔE centered on the line energy.

The range in sensitivity for MAX-NCTseg in addition includes the two choices for treating energy deposits in BRDLs, which may be ignored or used as additional veto, and are given for the optimal choice of SRDLs in each case. If energy deposits in BRDLs are ignored, for the 511 keV line it is best to use all five detector layers; for the 847 keV lines there is little difference between using three, four, or five layers (values are quoted for five layers). If BRDLs are used as additional veto the sensitivity can be slightly improved. It is then best to use only three detector layers in this case for both the 511 keV and the 847 keV lines. In either case the optimal central pixel radius is about 1.1 cm.

For MAX-NCTcompt the best radial size of the detector region where the first interaction needs to occur is slightly larger than for MAX-NCTseg; values range between 1.2 and 1.5 cm, depending on the details of the event selections. The achieved sensitivity depends only weakly on the choice of detector layers in which the first inter-

action needs to occur. It seems that restricting the first interaction to the top four layers is best.

As can be seen from Table 1, the Compton detector concept MAX-NCTcompt offers the best sensitivity for each of the three lines. In order to illustrate fundamental performance characteristics such as detection efficiency or background rejection, Table 2 summarizes the photopeak efficiencies and the background count rates corresponding to the choices for energy band, detector layers, and event selections that optimize the sensitivity for each of the three detector concepts and all three lines under study. The ranges for the MAX-NCTseg concept reflect the two different treatments of energy deposits in BRDLs (the lower and upper bounds are obtained if BRDLs are treated as additional veto or ignored, respectively). The photopeak efficiencies for MAX-NCTseg do not fall far short of those obtained with MAX-TGRS. Differences are due to the fact that photons can more easily escape MAX-NCTseg than MAX-TGRS, and that only a fraction of the incident photons interacts in one of the central pixels of the segmented MAX-NCTseg detectors. In contrast, the MAX-NCTcompt photopeak efficiency is much smaller. For this concept the rather low photopeak efficiency is due to the severe event selections, which result in many source events being rejected. Nevertheless, the MAX-NCTcompt concept offers the best sensitivity because of its superior capabilities for rejecting instrumental background, as can be seen in Table 2.

4. Summary and conclusion

We have used *ab initio* Monte Carlo simulations to compare the performance of three different Ge detector concepts for the MAX Laue lens gamma-ray telescope: a standard co-axial detector, a stack of segmented detectors, and a Compton camera consisting of a stack of strip detectors. The performance was assessed for an on-axis point source in three different gamma-ray lines: narrow lines at 511 keV and 847 keV, and a broadened (3% FWHM) line at 847 keV.

We find that the Compton detector concept MAX-NCTcompt offers the best sensitivity for each of the three lines. The Compton concept also offers other unique advantages over the other two concepts. Because of their fine spatial resolution, the detectors of a Compton camera are ideally suited to follow the inevitable small excursions of the focal spot on the detector surface due to residual relative motions of the lens and detector spacecraft; with a Compton camera one could also adjust the size of the focal spot to the requirements of a given observation during data analysis. The fine spatial resolution necessary for Compton detectors is also required if the limited imaging capabilities of a Laue lens are to be exploited, e.g. to separate close point sources or to study the morphology of slightly extended emission such as that from Galactic supernova remnants. Finally, the complementary characteristics of a Laue lens and of a Compton detector with respect to photon polarisation render their combination a

powerful polarimeter. At nuclear line energies a Laue lens does not change the polarisation of the diffracted photons (Halloin & Bastie 2006; Halloin 2006), while a Compton detector is intrinsically ideally suited for performing polarimetry because of the azimuthal variation of the scattering direction for linearly polarized photons (Lei et al. 1997). The combination of a Laue lens with a Compton detector will thus open a new observational window on many gamma-ray sources in which strong magnetic fields are present, such as pulsars, or on jets expelled by compact, accreting objects. We therefore conclude that a Compton camera is the most promising detector concept for MAX. We expect this conclusion to apply not only to the three gamma-ray lines studied here, but to all Laue lens gamma-ray telescopes proposed for the nuclear line region, such as the Gamma-Ray Imager (GRI, Knödlseider 2006).

Although not the primary focus of this study, it is still worth pointing out that even with a rather conservative design of the Compton camera that leaves still ample room for improvement, narrow line sensitivities of about 10^{-6} ph cm $^{-2}$ s $^{-1}$ are possible with a relatively small mission such as MAX – an improvement over the currently best gamma-ray spectrometer SPI onboard the INTEGRAL observatory of more than an order of magnitude.

There are many aspects in which the Compton camera studied here can be improved. First steps towards optimizing the design of the MAX-NCTcompt detector are presented in a companion paper by Wunderer et al. (2006b) (there, MAX-NCTcompt is referred to as the SMALL design). Possible improvements include a revised design of the BGO veto shield to decrease the instrumental background contribution of cosmic diffuse photons, the reduction of passive materials around the Ge wafers (passive material is a source of instrumental background and in addition reduces the photopeak efficiency because some fraction of the source photon's energy might be deposited there), the careful selection of passive materials used (e.g. elemental composition), the optimization of the geometry and the spatial and spectral resolution of the Ge detectors to increase the photopeak efficiency, or improvements of event reconstruction algorithms. Efforts to optimize the performance of a Compton detector for Laue gamma-ray lenses are ongoing (see e.g. the companion paper by Wunderer et al. 2006b) and will be reported in future publications.

References

- Abrsimev, N., et al., 2006, these proceedings
- Barrière, N., et al., 2006, these proceedings
- Boggs, S.E., et al., 2006a, New Astron. Rev., in press
- Boggs, S.E., et al., 2006b, these proceedings
- Brun, R., 1995, GEANT Detector Description and Simulation Tool, CERN Program Library Long Writup W5013, <http://wwwinfo.cern.ch/asd/geant/>
- Courtois, P., et al., 2006, these proceedings
- Gruber, D.E., et al., 1999, ApJ, 520, 124

- Halluin, H., et al., 2004, in *Proc. of the SPIE*, 5168, 471
- Halluin, H., 2006, these proceedings
- Halluin, H., & Bastie, P., 2006, these proceedings
- Kanbach, G., et al., 2004, *New Astron. Rev.*, 48, 275
- Kippen, M., 2004, *New Astron. Rev.*, 48, 221
- Knödlseider, J., 2006, these proceedings
- Lei, F., et al., 1997, *Space Sci. Rev.*, 82, 309
- Lonjou, V., et al., 2005, *NIM A*, 554, 320
- Lund, N., 1992, *Exp. Astron.*, 2, 259
- McConnell, M.L., & Kippen, R.M., 2004, AAS, HEAD Meeting #8, #41.01
- Moskalenko, I., et al., 2002, *ApJ*, 565, 280
- Owens, A., et al., 1995, *Space Sc. Rev.* 71, 273
- Prantzos, N., 2005, in *Proc. of 5th INTEGRAL Science Workshop* (ESA SP-552), 15
- Schönfelder, V., et al., 1993, *ApJS*, 86, 657
- Smither, R.K., et al., 1995, *Exp. Astron.*, 6, 47
- Smither, R.K., et al., 2006, these proceedings
- von Ballmoos, P., et al., 2004, *New Astron. Rev.*, 48, 243
- von Ballmoos, P., et al., 2006, these proceedings
- Weidenspointner, G., et al., 2003, *A&A*, 411, L113
- Weidenspointner, G., et al., 2005, *ApJS*, 156, 69
- Weidenspointner, G., 2006, in *Proc. of Population of High Energy Sources in Galaxies* (230. IAU Symposium), eds. E.J.A. Meurs and A. Fabbiano, in press
- Wunderer, C., et al., 2004, in *Proc. of 5th INTEGRAL Science Workshop* (ESA SP-552), 913
- Wunderer, C., et al., 2006a, *New Astron. Rev.*, in press
- Wunderer, C., et al., 2006b, these proceedings
- Zoglauer, A., 2005, *First Light for the Next Generation of Compton and Pair Telescopes* (dissertation), TU München
- Zoglauer, A., et al., 2006, *New Astron. Rev.*, in press